

# Formation Control with Area Constraints for Omnidirectional Mobile Robots

Diego I. Torres<sup>1[0009-0006-5535-2531]</sup>, Alma Y. Alanis<sup>1[0000-0001-9600-779X]</sup>,  
and Jorge D. Rios<sup>1[0000-0001-7565-0874]</sup>

Centro Universitario de Ciencias Exactas e Ingenierías, Universidad de Guadalajara,  
Guadalajara 44430, Mexico

**Abstract.** A consensus-based formation control strategy with area constraints and collision avoidance is used on omnidirectional mobile robots for testing flexibility and robustness. This control law integrates a vertex-tension function for collision avoidance problem. Simulations are presented using CoppeliaSim<sup>®</sup> from Coppelia Robotics AG, 8049 Zurich, Switzerland and the default omnidirectional model included.

**Keywords:** Signed area constraints · Omnidirectional-drive robots · Multi-robot systems · Collision avoidance · Formation control.

## 1 Introduction

Collaborative and cooperative task are one of most popular advantages for multi-agent systems, such applications can be cooperative transportation, search-and-rescue, collaborative exploration along with others [1, 2]. More precisely a multi-robot system can be described as a group of robots with the capabilities of communication, sensing and actuation, which can work together to solve a problem and archive a common goal. Formation control aim to drive a multi-robot system to archive certain patterns, most of the time formation control can be solved as a consensus problem, but there are many other ways to solve the formation problem [3, 4]. A consensus-bases formation control aims to converge all agents into a common value which defines pattern centroid [5].

Collision among agents are common when working with formation tasks of multiple agents, to solve this problem the most common approach is use of artificial potential field [6, 7], this method is unstable in presence of communication delays. Moreover, edge-weighted consensus-based formation control strategy can overcome these drawbacks by guaranteeing collision avoidance among agents by employing weighted graphs properties, allowing to adapt shape of formation to avoid collisions among robots. This work extends results presented in [8], where an edge-weighted formation control for differential mobile robots is presented, in which length of edges of the  $i$ th robot and  $j$ th robot are given by edge-tension function for collision avoidance and a signed area term to mitigate ambiguities in robot formation, the main focus is to implement the control law on different type of robots and a different environment to prove the robustness and flexibility

<https://doi.org/10.61728/AE20255022>



of the controller and its many advantages on multi-robot systems. In addition, inspiring to work with a wider variety of robots is another goal of this work and how they can be used to solve formation control problem.

This work addresses vertex-weighted consensus-based formation control with a control law that incorporates a vertex-tension function with a signed area term to consider constrains for omnidirectional robots, in past works edge-weighted consensus-based formation control with collision avoidance has been explore [12]. Vertex-tension functions aims to maintain agents of formation from colliding each other [10], by controlling the sign of the area of a triangle and the length of the sides we can add a constrain that mitigate ambiguities and avoid local minimum stagnation as well as helping with the desired formation shape, a desired shape can be construct be using a variety of triangles to form it. Another advantage of the signed area is the capability of perform formation control in a decentralized manner archiving the desired formation pattern in any initial position[11], we call this the sign area constrains. For the multi-robot system, omnidirectional mobile robots from simulation software CoppeliaSim<sup>®</sup> are used.

Omnidirectional mobile robots have non-conventional wheels allowing them to move along any direction in plane  $X$  and  $Y$  because of this, they have a good maneuverability. Furthermore, lineal velocities  $v_x$  y  $v_y$  and angular velocity  $\omega_z$  are control variables. In this paper, main focus are four wheeled configuration.

Main contributions of this paper can be summarized below: Given the vertex-weighted consensus-based formation control with area constraints and collision avoidance strategy and a desired formation, test proposed approach for an omnidirectional type of robot and prove the flexibility and robustness of this strategy. Test the efficiency under a different simulated environment.

This paper is organized as follows: Section 2, presents the kinematic model formulation of a holonomic omnidirectional mobile robot. Then, vertex-weighted consensus-based control design is included at Section 3. In Section 4, the experimental results are presented in CoppelisaSim<sup>®</sup> with graphics for the velocities and lengths of the edges. An analysis of the reported results are given in Section 5. Lastly, conclusions are presented in Section 6.

## 2 Kinematics Model Formulation

Case of study considers a set of  $N$  omnidirectional four wheeled drive robots, they are holonomic allowing all three degrees of freedom (DOF) to be controlled without restriction. A omnidirectional four wheeled drive robot model is illustrated in Fig. 1. For each mobile platform  $i$ , the robot pose is given by position  $(v_x, v_y)$  and orientation  $(\omega_z)$ , is a local framework  $F_o$ , with respect to a world frame  $FG$ .

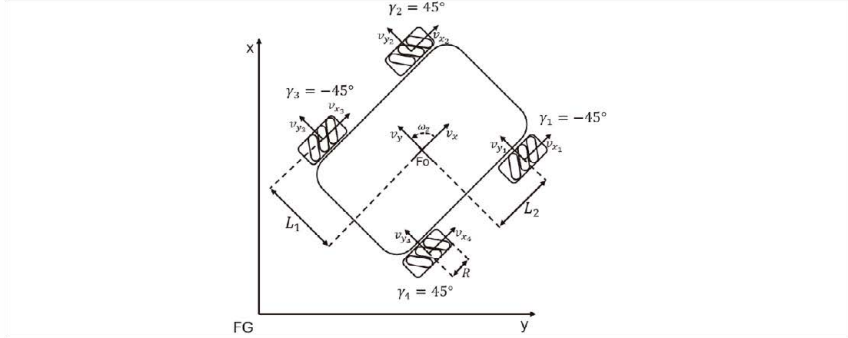


**Fig. 1.** Omnidirectional wheeled driven robot model.

each wheel  $i$  has a velocity  $v_{x_i}$  and  $v_{y_i}$ , rollers at an angle represented by  $\gamma_i$ ,  $R$  which denotes radius of wheels,  $L_1$  and  $L_2$  represent the distance between wheel axis and body center. Using the framework of each wheel, velocities of each component can be obtain and are represented in Eq. 1.

$$\begin{aligned}
 v_{x_1} &= v_1 + v_{r_1} \cos(45^\circ) & v_{x_3} &= v_3 + v_{r_3} \cos(45^\circ) \\
 v_{y_1} &= v_{r_1} \sin(45^\circ) & v_{y_3} &= -v_{r_3} \sin(45^\circ) \\
 v_{x_2} &= v_2 + v_{r_2} \cos(45^\circ) & v_{x_4} &= v_4 + v_{r_4} \cos(45^\circ) \\
 v_{y_2} &= -v_{r_2} \sin(45^\circ) & v_{y_4} &= v_{r_4} \sin(45^\circ)
 \end{aligned} \tag{1}$$

where  $v_i$  and  $v_{r_i}$  represents linear velocity of wheel  $i$  and rollers respectively. Based on local framework, the equations obtain for each wheel velocity are given by

$$\begin{aligned}
 v_{x_1} &= v_x - L_1 \omega_z & v_{x_3} &= v_x - L_1 \omega_z \\
 v_{y_1} &= v_y + L_2 \omega_z & v_{y_3} &= v_y - L_2 \omega_z \\
 v_{x_2} &= v_x + L_1 \omega_z & v_{x_4} &= v_x + L_1 \omega_z \\
 v_{y_2} &= v_y + L_2 \omega_z & v_{y_4} &= v_y - L_2 \omega_z
 \end{aligned} \tag{2}$$

based on Eq. 1 and Eq. 2 linear velocities can be expressed for each wheel  $v_i$  as a function of base frame as:

$$\begin{aligned}
 v_1 &= v_x - v_y - (L_1 + L_2) \omega_z \\
 v_2 &= v_x + v_y + (L_1 + L_2) \omega_z \\
 v_3 &= v_x + v_y - (L_1 + L_2) \omega_z \\
 v_4 &= v_x - v_y + (L_1 + L_2) \omega_z
 \end{aligned} \tag{3}$$

this is the inverse kinematic of a omnidirectional mobile robot with four wheels or inverse velocity solution [9] which can also be represented in matrix form as:

$$\begin{bmatrix} v_1 \\ v_2 \\ v_3 \\ v_4 \end{bmatrix} = \begin{bmatrix} 1 & -1 & -(L_1 + L_2) \\ 1 & 1 & (L_1 + L_2) \\ 1 & 1 & -(L_1 + L_2) \\ 1 & -1 & (L_1 + L_2) \end{bmatrix} \begin{bmatrix} v_x \\ v_y \\ \omega_z \end{bmatrix} \quad (4)$$

Therefore, the local kinematic of the four-wheeled omnidirectional model is given by Eq. 5.

$$\begin{bmatrix} v_x \\ v_y \\ \omega_z \end{bmatrix} = \frac{R}{4} \begin{bmatrix} 1 & 1 & 1 & 1 \\ -1 & 1 & 1 & -1 \\ 1 & 1 & 1 & 1 \\ -\frac{1}{L_1 + L_2} & \frac{1}{L_1 + L_2} & -\frac{1}{L_1 + L_2} & \frac{1}{L_1 + L_2} \end{bmatrix} \begin{bmatrix} v_1 \\ v_2 \\ v_3 \\ v_4 \end{bmatrix} \quad (5)$$

A transformation matrix show in Eq.6 is used to map velocities from local frame to global frame.

$$\begin{bmatrix} \dot{x} \\ \dot{y} \\ \dot{\theta} \end{bmatrix} = \begin{bmatrix} \cos(\theta) & -\sin(\theta) & 0 \\ \sin(\theta) & \cos(\theta) & 0 \\ 0 & 0 & 1 \end{bmatrix} \begin{bmatrix} v_x \\ v_y \\ \omega_z \end{bmatrix} \quad (6)$$

Replacing Eq. 5 in Eq. 6, inverse kinematic of the global frame is obtain, this is the kinematic of each omnidirectional robot

$$\begin{bmatrix} v_1 \\ v_2 \\ v_3 \\ v_4 \end{bmatrix} = \begin{bmatrix} \sqrt{2}\sin(\alpha) & -\sqrt{2}\cos(\alpha) & -(L_1 + L_2) \\ \sqrt{2}\cos(\alpha) & \sqrt{2}\sin(\alpha) & (L_1 + L_2) \\ \sqrt{2}\cos(\alpha) & \sqrt{2}\sin(\alpha) & -(L_1 + L_2) \\ \sqrt{2}\sin(\alpha) & -\sqrt{2}\cos(\alpha) & (L_1 + L_2) \end{bmatrix} \begin{bmatrix} \dot{x} \\ \dot{y} \\ \dot{\theta} \end{bmatrix} \quad (7)$$

where  $\alpha = \theta + \frac{\pi}{4}$ .

### 3 Edge-Weighted Formation Control

First, some concepts of graph theory are explain next to better comprehend robot undirected graph used for control law. An undirected graph with  $N$  elements is defined as  $G = (V, \mathcal{E})$ , where  $\mathcal{E} \subseteq V \times V$  is the edge set and  $V = \{v_i, i = 1, 2, \dots, N\}$  is the vertex set of cardinality  $N$ ,  $\mathcal{E}_k = (v_i, v_j)$  is the  $k$ th edge of  $G$  and represents bidirectional edge communication between agent  $i$  and  $j$ .

Then, vertex-tension function is define for every vertex  $v_i \in V$ , as proposed in [10] vertex-tension function is defined as

$$V_i = \sum_{j \in N_i} \alpha_{ij} \left( \coth \left( \frac{\|l_{ij}\| - \delta}{k_{ij}} \right) + \frac{1}{2} \|l_{ij}\|^2 - V_{ij}^{min} \right) \quad (8)$$

where  $N_i = \{\forall v_j \in V \mid (i, j) \in \mathcal{E}\}$  is a subset of neighbors of the  $i$ th robot, and  $K_{ij}$  is a constant that defines a related position of the minimum, for example, desired length between each couple of agents,  $\alpha_{ij}$  defines inter-robot influence,  $\delta$  is a safe distance parameter for collision avoidance,  $l_{ij} = p_i - p_j$  is an edge vector, where  $p_i$  and  $p_j$  are the state of the  $i$ th and  $j$ th agents respectively,  $V_{ij}^{min} > 0$  is defined as

$$\min_{\|l_{ij}\| > \delta} V_i = 0 \quad (9)$$

As proposed in [8] a connected graph is created in such way that each vertex  $v_i \in V$  is connected to, at least, one triplet  $(i, j, k)$ , where  $\{(i, j), (j, k), (k, i)\} \in \mathcal{E}$  and a signed area function is used for every triplet to avoid ambiguities and local minima. The set of all triplets  $(i, j, k)$  is denoted by  $T$ , if this set  $T$  is permuted in a cyclical manner, triangle form by the triplet is the same, the subsets of  $T_i$  can be defined as  $\{(i, j) \mid (i, j, k) \in T\}$  those are all triplets where the vertex  $v_i$  is involved. The triplet-tension function used for every vertex is defined in Eq. 10.

$$V_{T_i} = \sum_{(j,k) \in T_i} \frac{1}{2} K_{T_{ijk}} (S_{ijk} - S_{ijk}^*)^2 \quad (10)$$

where  $K_{T_{ijk}} \in \mathbb{R}$  and  $K_{T_{ijk}} > 0$  this gain allows for avoiding ambiguities and local minima, desired signed area is represented by  $S_{ijk}^*$  and current signed area is  $S_{ijk}$  which is defined as:

$$S_{ijk} := \frac{1}{2} \det \begin{bmatrix} 1 & 1 & 1 \\ P_i & P_j & P_k \end{bmatrix} \quad (11)$$

which denotes a triangle who is either positive or negative according to the ordering of  $P_i, P_j, P_k$  around the boundary of the triangle is counterclockwise, or clockwise [11].

A total potential function is defined based on Eq. 8 and Eq. 10.

$$V = \sum_{i=1}^N (V_i + V_{T_i}) \quad (12)$$

The total potential function  $V$  obtain before is the edge-weight function which is designed to ensure collision avoidance between agents  $i$  and  $j$ , if the  $\delta$  parameter is strictly greater than the distance  $\|l_{ij}\|$ . The distance between robots  $i$  and  $j$  is given by

$$\|l_{ij}\| = \delta + K_{ij} \operatorname{acsch} \left( \sqrt{K_{ij}} \right) \quad (13)$$

when this function reaches its minimum the magnitude of the edge vector becomes the specified as desired.

A gradient descent control law for every robot is defined so that the  $i$ th agent moves according to  $\dot{P} = -\frac{\partial V}{\partial P_i}$  which can be translate to Eq. 14

$$\dot{P}_i = U_{N_i} + U_{T_i} \quad (14)$$

where

$$U_{N_i} = - \sum_{j \in N_i} \alpha_{ij} \left( -\frac{1}{k_{ij} \|l_{ij}\|} \operatorname{csch}^2 \left( \frac{\|l_{ij}\| - \delta}{k_{ij}} \right) + 1 \right) (P_i - P_j) \quad (15)$$

$$U_{T_i} = - \sum_{(i,j) \in T_i} K_{T_{ijk}} (S_{ijk} - S_{ijk}^*) \begin{bmatrix} 0 & 1 \\ -1 & 0 \end{bmatrix} (P_j - P_k) \quad (16)$$

The Control Law in Eq. 14 is designed for holonomic robots. For a decentralized control, it is important to ensure that the information used is not accessible to a central unit, but to the robots and every vertex in the graph is part of at least one triplet. Since, signed area function described in Eq. 11 requires the global positions of  $P_i$ ,  $P_j$  and  $P_k$  for control. For decentralized control purposes this function can be expanded and express in relative position terms:

$$S_{ijk} = \frac{1}{2} (P_i - P_j)^T \begin{bmatrix} 0 & 1 \\ -1 & 0 \end{bmatrix} (P_i - P_k) \quad (17)$$

## 4 Experimental Results

The performance and flexibility of the formation control strategy design in [8] is verified with the use of four omnidirectional mobile robots simulated using CoppeliaSim<sup>®</sup> and four of preset omnidirectional robot model included in this software. Since omnidirectional robots are holonomic unlike differential robots we can use the conventional  $\dot{P}_i = [x_i, y_i]^T$ .

The desired formation aim in this paper is a rhombus shape, the parameters to form this shape are  $k_{ij}$  and  $S_{ijk}^*$ , where  $K_{ij}$  defines the distance between agents  $P_i$  and  $P_j$ , while  $S_{ijk}^*$  is the desired signed area. Formation control settings are briefly described,  $\delta$  which is the safety distance,  $\alpha$  which is the inner-robot influence and  $K_{T_{ijk}}$  which is signed area control gain for triplets. Parameters for each experiment are presented later for different distances of this shape.

First, a rhombus shape with edge distance  $\|L_{ij}\| = 1$ , the distance values to get that magnitude are defined as  $k_{ij} = 0.85175781$  and  $S_{ijk}^* = -0.43301$ , formation control parameters are  $\delta = 0.5$ ,  $\alpha = 1.0$  and  $K_{T_{ijk}} = 5.0$ . In Fig. 3. linear and angular velocities can be observed and how they converge, based on Fig. 4. we can observed the edge distances close to 1 with a small error between the different edges, while the formation is archive as shown in Fig. 2. the error, although small, is significant and can be improved.

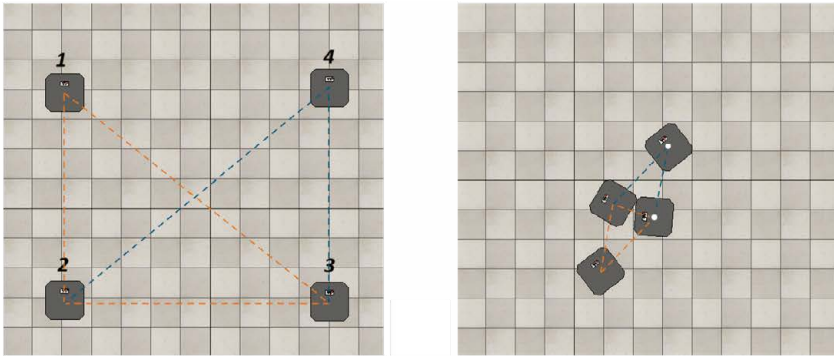


**Fig. 2.** Initial and final position of four omnidirectional robots for distance of 1.

In fig 2. we can see the arrange of the robots in their initial position an the connections between them, as well as the final rhombus shape and how the graph moved.

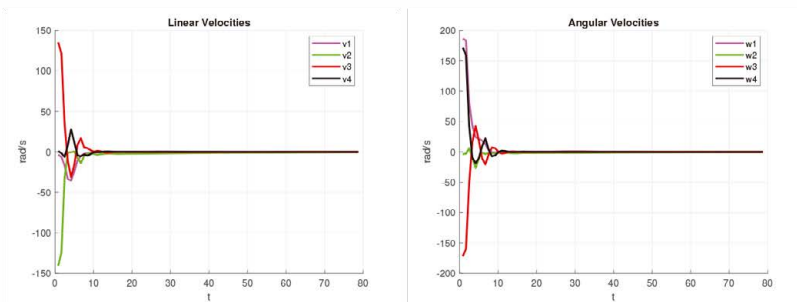


**Fig. 3.** Linear and angular velocities of each robot.

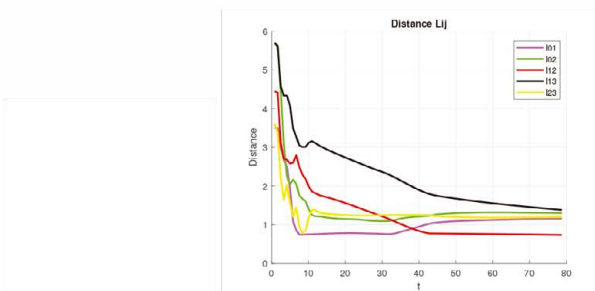


**Fig. 4.** Edge distance of each connection  $l_{ij}$  with a distance of 1.

In the next figures an increase on the distance was implemented for this the parameters used were  $k_{ij} = 8.5175781$  and  $S_{ijk}^* = -4.3301$ , for the formation control settings the parameters were  $\delta = 1.0$ ,  $\alpha = 1.0$  and  $K_{T_{ijk}} = 1.5$ , the results are shown in Fig. 2 where a clear bigger rhombus shape was archive.

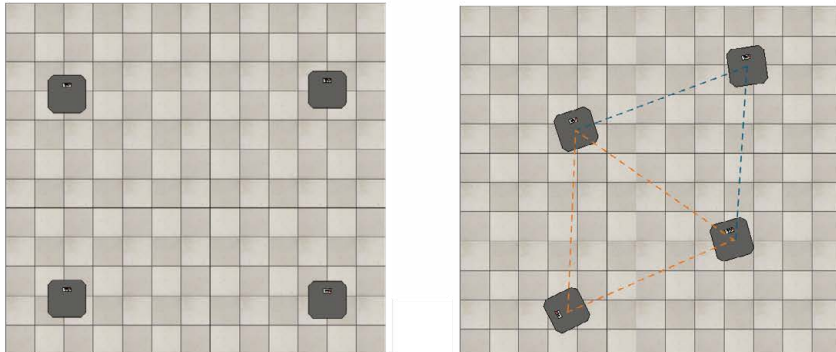


Fig. 5. Initial and final position of four omnidirectional robots with a bigger distance.

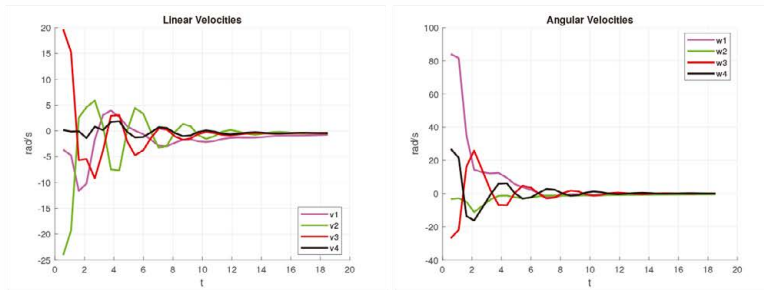


Fig. 6. Linear and angular velocities of each robot.

As expected the formation shape is archive with a better result than the obtain in Fig. 4, the distance between each edge converge with less error than the first example meaning it can be improve with a good selection of parameters, since this experiment was made in CoppeliaSim<sup>®</sup> another factor can be added since the experiment runs on a continuous timer this can be consider as an online experiment.

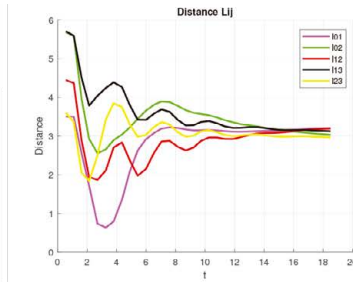


Fig. 7. Edge distance of the increased formation.

## 5 Discussion

The results obtained here prove the flexibility of the control law seen in [8] where the desired shape was achieved with a minimal error, while the results obtained here have been shown to contain an error. The proposed approach has many advantages in formation control with a variety of robots, with this paper we add the flexibility and robustness to that control law and how it works under an online simulation, also the capabilities of a holonomic robot using this method can be seen, since the controller shown in Eq. 14 is holonomic. The performance seen here was good, achieving the correct formation in under 15 seconds. A next step for this type of controller could be the experimentation of different types of robots like a three-wheeled omnidirectional robot or legged ones, also formation control mixing different types to solve this problem, the use of aerial mobile robots on a third-dimensional environment is another possible step in which they could incorporate the use of signed volume or use of robots with control law on a real-world task.

## 6 Conclusions

This paper addressed the implementation of an edge-weighted consensus-based formation control for omnidirectional four-wheeled driven robots in which robustness and flexibility are the objective of this work for a different mobile robot since some works in the past use this type of controller on a differential mobile robot, by achieving the desired formation with a small error in an environment close to real-world physics we can prove the efficiency of this type of controller for formation problems, since the controller is designed based on a graph topology and the use of signed area makes it so not all of the vertices are required to be connected, the results obtained here are satisfactory, proving the efficiency, robustness, and flexibility of this type of controller and how it can be used on different types of robots and different environments.

## References

1. Issa, B.A.; Rashid, A.T. A survey of multi-mobile robot formation control. *Int. J. Comput. Appl.* 2019, 181, 12–16.
2. Oh, K.K.; Park, M.C.; Ahn, H.S. A survey of multi-agent formation control. *Automatica* 2015, 53, 424–440.
3. Gong, X.; Liu, J.J.; Wang, Y.; Cui, Y. Distributed finite-time bipartite consensus of multi-agent systems on directed graphs: Theory and experiment in nano-quadcopters formation. *J. Frankl. Inst.* 2020, 357, 11953–11973.
4. Zhou, Y.; Liu, Y.; Zhao, Y. Prescribed-time Bipartite Consensus Formation Control for General Linear Multi-agent Systems. In *Proceedings of the IECON 2020 The 46th Annual Conference of the IEEE Industrial Electronics Society, Singapore, 19–21 October 2020*; pp. 3562–3567.
5. Jadbabaie, A.; Lin, J.; Morse, A.S. Coordination of groups of mobile autonomous agents using nearest neighbor rules. *IEEE Trans. Autom. Control.* 2003, 48, 988–1001.
6. Hu, J.; Wang, M.; Zhao, C.; Pan, Q.; Du, C. Formation control and collision avoidance for multi-UAV systems based on Voronoi partition. *Sci. China Technol. Sci.* 2020, 63, 65–72.
7. Xia, G.; Zhang, Y.; Yang, Y. Control Method of Multi-AUV Circular Formation Combining Consensus Theory and Artificial Potential Field Method. In *Proceedings of the 2020 Chinese Control And Decision Conference (CCDC), Hefei, China, 22–24 August 2020*; pp. 3055–3061.
8. Hernandez-Venegas, Ulises & Hernandez-Barragan, Jesus & Gómez Jiménez, Irene & Martínez-Soltero, Gabriel & Alanis, Alma. (2025). Vertex-Weighted Consensus-Based Formation Control with Area Constraints and Collision Avoidance. *Algorithms*. 18. 45. 10.3390/a18010045.
9. Doroftei, I., Grosu, V., & Spinu, V. (2007). Omnidirectional mobile robot-design and implementation (pp. 511-528). London, UK: INTECH Open Access Publisher.
10. Falconi, R.; Sabattini, L.; Secchi, C.; Fantuzzi, C.; Melchiorri, C. Edge-weighted consensus-based formation control strategy with collision avoidance. *Robotica* 2015, 33, 332–347.
11. Anderson, B.D.; Sun, Z.; Sugie, T.; Azuma, S.i.; Sakurama, K. Formation shape control with distance and area constraints. *IFAC J. Syst. Control* 2017, 1, 2–12.
12. Hernandez-Barragan, J., Hernandez, T., Rios, J. D., Perez-Cisneros, M., & Alanis, A. Y. (2023). Edge-Weighted Consensus-Based Formation Control with Collision Avoidance for Mobile Robots Based on Multi-Strategy Mutation Differential Evolution. *Mathematics*, 11(17), 3633. <https://doi.org/10.3390/math11173633>